Concentration dependences of the transport coefficients of rod-like molecules in narrow slit-shaped pores

Yu. K. Tovbin and A. B. Rabinovich*

State Scientific Center "L. Ya. Karpov Physicochemical Research Institute," 10 ul. Vorontsovo pole, 103064 Moscow, Russian Federation. Fax: +7 (495) 975 2450. E-mail: tovbin@cc.nifhi.ac.ru

The concentration dependences of the label transport and shear viscosity coefficients for rod-like molecules in slit-shaped pores were studied. The calculations were carried out using the lattice gas model, which describes a broad range of fluid concentrations (from the gaseous to the liquid state) and temperatures (including the critical region). In the calculation of the local distributions of mixture components in the equilibrium states, lateral interactions were taken into account. The translational and rotational motions of molecules were described in terms of the transition state theory for nonideal reaction systems, which took into account the influence of neighboring molecules on the height of the activation barrier. The model equations reflect the pronounced anisotropy of the distribution of system components along the normal to the pore wall surface and ordering effects of molecules along various directions.

Key words: adsorption, quasichemical approximation, label transport coefficient, shear viscosity coefficient, lattice gas model, monolayer adsorption, rod-like molecules, slit-shaped pore.

In many processes[1—3] that take place in porous solids, an important role belongs to the transport of molecules. Porous bodies with a developed surface are known to contain narrow pores in which the wall potential gives rise to an anisotropic distribution of molecules over the cross-section, which influences the physical state of the fluid and the mechanism of its transport. With respect to inert gases and simple molecules like nitrogen, oxygen, or methane, up to 15 nm wide pores are classified as narrow.[4]

Fluxes of molecules in narrow pores are analyzed by molecular dynamics technique,[5—8] which is, however, highly labor-consuming. Previously,[9,10] an alternative approach based on the lattice gas model (LGM) has been proposed for adapting the hydrodynamic transport equations to description of the molecular transport in narrow pores.[11,12] The transport equations constructed in terms of this model[9,10] take into account two key features of the molecular distribution in narrow pores. The first one is the high anisotropy of molecular distribution along the normal to the pore wall caused by adsorption forces. In addition, in the presence of capillary condensation, anisotropy along the pore axis arises at the gas—liquid interface.

This work extends the equations describing the rates of thermal motion of the components in mixtures of spherical molecules whose size is equal to dimensions of a site in the LGM[11] to mixtures of rod-like molecules of various lengths. The rates of thermal motion of rod-like molecules are considered within the framework of the absolute reaction rate theory for nonideal systems.[11,12] The equations of the theory should reflect the mutual orientation of rods with different size and the possibility of their ordered state and also take into account the intermolecular interactions of components in dense nonuniform phases inside the pores.

Similar problems exist for solutions and liquid crystals in the bulk phase.[13—15] Rod-like molecules represent the simplest case of molecules shaped like rectangular parallelepipeds.[16,17] The equilibrium adsorption theory of molecules shaped like rectangular parallelepipeds in narrow slit-shaped pores was described in previous publications.[16,17] The known potential functions for intermolecular interactions and for interactions of a molecule with the pore walls served as the input information.[13,18—20] The lateral interactions were included in the calculation of the local distributions of mixture components in the equilibrium states in the approximation of isolated contacts. This approximation has been used previously[13] to calculate the equilibrium characteristics for bulk phases and for liquid—vapor interface and to analyze the rates of chemical reactions,[21] and the corresponding calculations were reported.[22,23] Equations for the calculation of migration rates of rod-like molecules have also been reported.[24] The lattice gas model for rod-like molecules has been reported previously;[24,25] hence, it is not described in this publication. The number of nearest neighbors in the

Published in Russian in *Izvestiya Akademii Nauk. Seriya Khimicheskaya,* No. 9, pp. 1485—1494, September, 2006.

1066-5285/06/5509-1539

lattice $z = 6$, the rod length L was taken to be equal to the lattice constant. Recall that the index (or the sort) of a molecule is determined by its number as a system component and orientation.

Elementary motion of the molecule. The elementary motions of the rods are related either to a shift of the center of gravity or to rotation with respect to the center of gravity. A shift of the center of gravity of the rod i without a change in the orientation λ_i is regarded as translational movement (jump) between neighboring sites f and g. The density of rarefied gases is usually $\theta \le 10^{-3}$, hence, the free path of a molecule is many times greater than the pore width. In the liquid phase, the free path is commensurable with the molecule dimensions. To describe the properties of both the rarefied gas and dense liquid phases, LGM does not use the free path concept. Instead, the model operates the notion of migration probability or jump rate $U_{fg}^{i\nu}$ of particle i from site f by distance χ into free cell ν of site g, which is applicable over the whole density θ range from 10^{-4} to 1 (see Refs 11, 12).

The reorientations of particle i during its rotation relative to the center of inertia or the pore wall occur in different ways. In the former case, rotation can be considered independently of the translational motion of the rod if the reference point of the moving coordinates coincides with the center of inertia of the rod. In the latter case, both types of motion are interrelated.

In the rotation of rods, we will consider only the nearest discrete orientational states between which direct rotations (transitions) are possible.

For example, let f be the central site of a rod of sort i and g be the adjacent site, such that the direction of the fg bond coincides with the direction of the rod. Upon the rotation, the central site of the rod remains invariable. Only the direction of the rod changes and, hence, the sort; it will be designated by index k. The character g_1 stands for the site next to f such that the direction of the fg_1 bond coincides with the new direction of the rod.

The discrete transitions from the fg to fg_1 bond in which the angle φ between the vectors of the initial and new directions does not exceed 90° are regarded as direct transitions. All rotations of rod i will be classified into rotations with angles greater and smaller than $\varphi/2$.

In the former case, one deals with "internal" rotation. In this case, the index i and the orientation λ_i are retained; the molecule "rocks" relative to the center of gravity with slight deviations from the orientation λ_i. In the latter case, the process is the "external" rotation where the index i of the molecule is replaced by k and the orientation λ_i is replaced by λ_k (see Ref. 25). Let $W_f(i \to k)$ be the average rate of the elementary change in orientation of the rod i located in site f to rod k whose center of gravity remains in the same site f. It is evident that the coordinate of the geometric center of a polyatomic molecule does not coincide, in the general case, with the coordinate of the center of gravity, which additionally complicates the site indexing in the description of rod dynamics.

The presence of impermeable pore wall affects the molecular motion in a dual way: first, the wall restricts the rotation angles around the center of gravity for molecules located near the wall; second, molecules can change the orientational states through rotation around the surface atoms (or functional groups). The molecules are characterized by momentum of inertia counted off from the contact point with the surface. The rotational motion of this sort, together with the molecule orientation change the position of the center of inertia, and their contribution should be taken into account in analysis of the fluxes that shift the centers of inertia.

Calculation of the rates. The rates of elementary motions will be described in terms of the transition state theory for nonideal systems. Previously, the rotation of large molecules has not been considered within the LGM. Let us find the expression for the rate of rotational motion using the idea of the transition state theory according to which the number of activated complexes (AC) per unit volume θ^* determines the rate of the elementary process $U = \theta^* \nu$, where ν is the frequency of crossing the activation barrier (s^{-1}). For the rotational motion, $\nu = u_r/\varphi$, where u_r (rad s^{-1}) is the average angular rate of rotation during passage through the activation barrier, φ is the arc length in radian. The average rate of rotation in a specified direction is expressed as $u_r = (kT/2\pi I^*)^{0.5}$, where I^* is the AC momentum of inertia.[26] The AC concentration on the barrier top can be expressed as follows: $\theta^* = \theta F_r$, where θ is the AC concentration after replacement of one degree of freedom of the rocking type motion, similar to the vibration type motion, by rotational motion, $F_r = (2\pi I^* kT)^{0.5}\varphi/h$. From this, $U = \theta kT/h$. By introducing, in a usual way, the specific rate of an elementary process $K_i = U/\theta_i$ for the motion of rod I, we get $K_i = \theta kT/(h\theta_i)$. This derivation is fully analogous to the derivation of the expression for translational motion[27] for which $\nu = u_t/\delta$, where $u_t = (kT/2\pi m^*)^{0.5}$ is the average rate of motion of an AC with the mass m^* and δ is the length of the activation barrier. Meanwhile, for translational motion $\theta^* = \theta F_t$, $F_t = (2\pi m^* kT)^{0.5}\delta/h$; hence, $K_i = \theta kT/(h\theta_i)$.[27]

The ratio $\theta/\theta_i = F^*/F_i$ is expressed[11,12,26,27] in terms of the partition function for AC (F^*) and for the molecule in the ground state (F_i), which can be used to express the kinetic constant for elementary motion in the gas phase in the usual form $K_i = kTF^*/(F_i h)$. This formula has the same form for any type of motion of the molecule (translational or rotational). The type of molecular motion dictates the particular expressions for the partition functions of the AC and of the molecule in the ground state. For the rotational motion in a rarefied phase, $F^*/F_i = F_r$.

For nonideal reaction systems, the expression for the F^*/F_i ratio becomes more complicated, because the influ-

ence of neighboring molecules must be taken into account. This influence is manifested through lateral interactions and through the vacancy regions in the dense phase, which allows the translational or rotational type of the elementary motion to occur.

For single-site migrating particles, the vacancy region consists of at least one neighboring vacancy to which the molecule migrates.[11,12] Migration by longer distances $\chi > 1$ requires a vacancy region that would provide a jump trajectory comprising a sequence of χ vacancies. In the case of single-site rotating particles, a change in orientation is considered only as a change in the intrinsic state of particles. This type of motion does not involve vacancies.[11,12]

Different elementary motions of a rod require different vacancy regions. When the center of inertia is displaced by one site, the vacancy regions coincide with the $S_{m\gamma}$ values: one vacancy ($S_{m\gamma} = 1$) should be available along the direction of motion of the rod longer axis and L vacancies ($S_{m\gamma} = L$) should be available along the direction of motion of the rod lateral face (Fig. 1, *a*). If the rod shifts by distance $\chi > 1$, the vacancy region covers a trajectory comprising a sequence of χ-long vacancies, the number of vacancies across the trajectory cross-section being $S_{m\gamma}$.

The vacancy region for the $i \to k$ rotation consists of a full number of vacant sites crossed by the rod during transition from state i to state k. We will designate it by $S(i \to k)$. In the starting and final positions, the rod blocks L vacancies; hence, $S(i \to k) > L$ (see Fig. 1, *b*). When the molecule rotates with respect to the pore wall, the vacancy region should comprise $S_w(i \to k)$ vacancies that ensure rotation of the rod along some arc from state i to k. In the general case, $S(i \to k) > S_{m\gamma}$ and $S_w(i \to k) > S(i \to k)$.

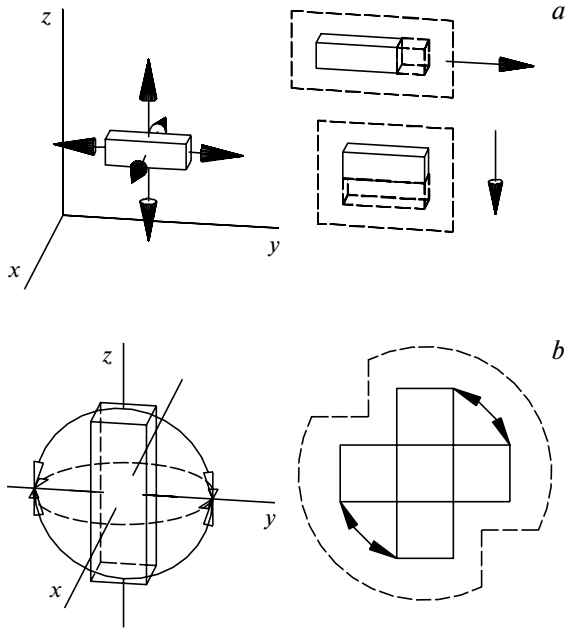

Fig. 1. Types of motions (*a*) and rotations (*b*) of the rods in Cartesian coordinates. The arrows mark the direction of rod movement along the Cartesian axes or during rotation of the molecule, the dashed lines show the vacancy regions required for rod movement and the long-dashed lines are neighboring molecules that influence the elementary migrations.

The rates of thermal motion

Translational motion of particles. The average rate of the translational motion of rods from site f to vacant site g by distance χ is given by[11,12,21,22]

$$U_{fg}^{i\nu}(\chi) = K_{fg}^{i\nu}(\chi) V_{fg}^{i\nu}(\chi), \quad (1)$$

$$K_{fg}^{i\nu}(\chi) = (2\pi m_i \beta)^{-0.5} \exp[-\beta E_{fg}^{i\nu}(\chi)]/\chi,$$

$$V_{fg}^{i\nu}(\chi) = \langle \theta_{fg}^{i\nu} \rangle \Lambda_{fg}^{i},$$

$$\langle \theta_{fg}^{i\nu} \rangle = \theta_{f(1)}^{i\nu *} \prod_{l} t_{l(l+1)}^{\nu\nu *},$$

where $K_{fg}^{i\nu}(\chi)$ is the kinetic constant of the jump expressed through the average rate of the thermal motion of particle i; m_i is the mass of particle i; $E_{fg}^{i\nu}(\chi)$ is the activation energy of the jump, which depends on the distance from the wall and on the direction of rod movement. Away from the pore wall potential, the activation energy is equal to zero.

The dependence of the particle migration rate on the concentration is expressed by the multiplier $V_{fg}^{i\nu}(\chi)$ in which two factors are taken into account.

1. Probability of the existence of free trajectory $\langle \theta_{fg}^{i\nu} \rangle$, which rules out blocking of the trajectory from site f to site g by other particles; this trajectory comprises sites f, $(1) = f + 1$, $(2) = f + 2$, *etc.* up to site g. The trajectory has $S_{i\gamma}$ vacancies in the cross-section (this is marked by an asterisk *). The direction of motion from site f to site g for a specified rod orientation i unambiguously determines the full size of the vacancy region consisting of a trajectory part of length $\chi - 1$ (this is described by multipliers for l in the expression for $\langle \theta_{fg}^{i\nu} \rangle$) and a vacancy region for the shift of the rod by one site. If $\chi = 1$, $g = (1)$, and only the first multiplier $\theta_{f(1)}^{i\nu *}$ remains in the expression for $\langle \theta_{fg}^{i\nu} \rangle$.

2. The function Λ_{fg}^{i} taking into account the effect of lateral interactions of surrounding particles. These particles are arranged around the whole trajectory from site f to site g with the cross-section $S_{i\gamma}$ along which the particle i migrates. According to the contact model,[21] the quasichemical approximation for pairs of contacts gives

$$\Lambda_{fg}^{i} = A_1^i \cdot B_1^{\nu}, \quad (2)$$

$$A_1^i = \prod_{k=1}^{\Pi_i} {}^{*} \sum_{j=1}^{\Phi+1} \sum_{n=1}^{\Pi_j} t_{ij}^{kn}(fh) \exp(\beta \delta \varepsilon_{ij}^{kn}),$$

$$B^{v}_{l} = \prod_{d=1}^{\Pi_v} {}^{*} \sum_{j=1}^{\Phi+1} \sum_{n=1}^{\Pi_j} t_{vj}^{dn}(gh) \exp(\beta\delta\varepsilon_{vj}^{dn}),$$

where l corresponds to straight line motion, $\delta\varepsilon_{ij}^{kn} = \varepsilon^{*}_{ij}{}^{kn} - \varepsilon_{ij}^{kn}$, and $\varepsilon^{*}_{ij}{}^{kn}$ is the energy parameter for the interaction of contact k of molecule i in the activated state during migration with the neighboring contact n of molecule j located in site h. In the first product, the character h refers to neighbors j of the central particle i. The asterisk at the first product sign means that the contacts adjacent to the vacancy region in which particle i migrates toward site g are excluded from the set of contacts $k \in \Pi_i$ of molecule i. The asterisk at the second product sign indicates that only contacts of the proper particle i migrating toward site f are excluded from the set of contacts $d \in \Pi_v$ of the vacancy region (in the second product, the sign h refers to the neighbors that surround the vacancy region).

The average rate of motion between sites f and g well be designated by $w_{fg}{}^{i}$; it is related to the average jump rate $U_{fg}{}^{iv}(\chi)$ in the following way:

$$w_{fg}{}^{i} = \chi U_{fg}{}^{iv}(\chi)/\theta_f^{i}, \qquad (3)$$

where χ is the average jump rate.

The rotation of particles relative to the center of inertia. Let particle i rotate around its principal rotation axes that pass through the inversion center in site f. In the condensed phase, the particle rotates after it has attained the required activation energy of rotation and has gained the angular momentum in the required direction as a result of thermofluctuation perturbations of the medium. In addition, the rotation of a molecule is affected by the total external moment of the forces acting on the given particle i due to the adsorption potential. The reorientation rate can be described by analogy with the traditional method[11,12] without specifying the particular contributions of collisions with neighboring particles. In this case, the reorientation rate $i \to k$ of a rod in site f is given by

$$W_f(i \to k) = K_f^{i}(i \to k) V_f^{i}(i \to k), \qquad (4)$$

$$K_f^{i}(i \to k) = (2\pi I_{ik}\beta)^{-0.5} \exp[-\beta E_f^{i}(i \to k)]/\varphi,$$

$$V_f^{i}(i \to k) = \langle \theta_f^{i}(i \to k) \rangle \Lambda_f^{i}(i \to k),$$

$$\langle \theta_f^{i}(i \to k) \rangle = \theta_f^{iv*} \prod_{l} t_{l(l+1)}^{vv*}.$$

Here $K_f^{i}(i \to k)$ is the kinetic constant for reorientation of molecule m from state i ($i \rightleftharpoons m, \lambda_i$) to state k ($k \rightleftharpoons m, \lambda_k$); $E_f^{i}(i \to k)$ is its activation energy; I_{ik} is the principal momentum of inertia of particle i corresponding to its rotation around the center of inertia with transition to state k; for rods $I_{ik} = I$. The expression for I depends on the rod structure. For small-size molecules, an atomic discrete model of the rod should be used, in which $I = \sum_{A \neq B} m_A m_B L_{AB}^2 / M$, where L_{AB} is the distance between atoms A and B.[28] For large particles, macroscopic description should be used in which $I = ML/12$, where M is the mass of the rod, L is the rod length.[28]

As in the above-described case, the concentration dependence of the reorientation rate $i \to k$ ($V_f^{i}(i \to k)$) takes into account two factors.

1. The probability $\langle \theta_f^{i}(i \to k) \rangle$ of the existence of vacancy region $S(i \to k)$ whose size and shape are sufficient for reorientation $i \to k$ to occur. Formally, the equation for this probability in expression (4) differs from formula (1) by the absence of an index for site g and the designation for the vacancy in it, because the rotation occurs with respect to site f.

2. The function $\Lambda_f^{i}(i \to k)$, which describes the influence of the surrounding particles on the reorientation of particle i. For rotational motion, expression (2) is replaced by a similar one

$$\Lambda_f^{i}(i \to k) = A_r^{i} \cdot B_r^{v}, \qquad (5)$$

$$A_r^{i} = \prod_{k=1}^{\Pi_i} {}^{*} \sum_{j=1}^{\Phi+1} \sum_{n=1}^{\Pi_j} t_{ij}^{kn}(fh) \exp(\beta\delta\varepsilon_{ij}^{kn}),$$

$$B_r^{v} = \prod_{d=1}^{\Pi_v} {}^{*} \sum_{j=1}^{\Phi+1} \sum_{n=1}^{\Pi_j} t_{vj}^{dn}(fh) \exp(\beta\delta\varepsilon_{vj}^{dn}).$$

As in the above-considered case, the character h in the first product refers to neighbors j of the central particle i in site f, whereas in the second product, this refers to neighbors that surround the vacancy region at the end of the rotation trajectory. The asterisk at the first product sign means that the contacts adjacent to the vacancy region $S(i \to k)$ in which rotation from particle i to particle k takes place are excluded from the set of contacts $k \in \Pi_i$ of molecule i. The asterisk at the second product sign indicates that contacts with the central particle k are excluded from the set of contacts $d \in \Pi_v$ of the vacancy region $S(i \to k)$.

The rotation of particles relative to pore walls. On rotation of a molecule relative to the wall, its center of inertia shifts, *i.e.*, the shift and rotation of the rod are joint processes. In the description of the rod rotation relative to the pore wall, expressions (4) and (5) for the rates of elemental rotations are modified. Only the shape of the vacancy region $S_w(i \to k)$, which ensures rotation of the rod along some arc from the state i to k changes, and the momentum of inertia of the molecule $I_{ik}{}^{w}$ relative to the wall atoms is used in the expression for the reorientation rate $K_{fw}{}^{i}(i \to k)$, instead of I_{ik} used in formula (4).

The average thermal rate of the translational motion from site f to free site g is expressed in terms of the rotation rate with respect to the wall:

$$w_{fg}{}^{i} = \chi_{fg}{}^{i}(i \to k) W_{fw}(i \to k)/\theta_f^{i}, \qquad (6)$$

where $\chi_{fg}(i \to k)$ is the shift of the center of inertia of particle i projected on the fg bond upon the rotation $i \to k$; the

function $W_{fw}(i\to k)$ is described by modified formulas (4) and (5) using the values $K_{fw}^{i}(i\to k)$ and $S_w(i\to k)$.

The inclusion of constraints on the rotation angles in the near-wall layers caused by pore wall impermeability changes the shape and decreases the size of the vacancy space needed for the given type of rotation. Then the function Λ_{fg}^{i} in Eq. (1) does not contain contributions of the contacts of rods with wall atoms. The interactions with the wall are taken into account in the expression for the activation energy $E_{fg}^{iv}(\chi)$.

Transport coefficients

Translational label transport coefficient. The rate of thermal motion of the particles gives the expression for a local label transport coefficient during translational motion, which depends on the mixture density and the intermolecular interaction of the labeled particles with all neighbors. For a labeled particle of sort i, the following expression holds:

$$D_{fg}^{i*} = z_{fg}^{*}\chi^2 U_{fg}^{iv}(\chi)/\theta_f^i, \qquad (7)$$

where $z_{fg}^{*}(\chi)$ is the number of possible jumps between neighboring sites f and g.

Let us designate the label transport coefficient for translational motion by D_l^{ij}, where the first superscript characterizes the rod orientation $i = X, Y, Z$ and the second one shows the motion direction $j = X, Y, Z$. The movement along the longer axis (for $i = j$) will be called motion of the first type, while movement across the longer axis (for $i \neq j$), will be termed motion of the second type.

Calculation conditions and the bulk phase. The distribution equilibria of rod-like molecules required for calculating the dynamic characteristics have been considered previously.[25] Apart from the isotropic distribution, rod-like molecules have ordered distributions along the distinguished axis i ($i = X, Y, Z$). The ordering effect is observed for rods with length $L > 3$ when the fluid volume fraction or density ω is greater than certain $\omega = \omega_{bif}$. At low ω values, all orientations of the molecules are equivalent, *i.e.*, molecules are distributed isotropically. The algebraic system of equations[25] that describes the distribution of molecules has only one solution: $\omega_i = \omega/3$, $i = X, Y, Z$. With an increase in ω on passing through the ω_{bif} value corresponding to ordering of the rods, additional solutions appear to this system of algebraic equations.[25]

In the plot, this is manifested as an abrupt transformation of the curve for ω_i *vs.* fluid density ω into two curves. This is due to the fact that up to the density $\omega = \omega_{bif}$, the partial fillings ω_X and ω_Y coincided and were responsible for a single curve. At the point $\omega = \omega_{bif}$ they were converted jumpwise into two different curves ω_X and ω_Y, where $\omega_X > \omega_Y$. A similar phenomenon has been observed for the transport coefficients considered below.

Additional solutions appear as a step of partial densities in the point $\omega = \omega_{bif}$ called the bifurcation point. The physical meaning of the appearance of additional solutions is that the isotropic distribution of the fluid molecules becomes unfavorable. The transition into a new physical state with molecular ordering along an X, Y, or Z axis corresponds to a free energy minimum. The ω_{bif} value depends on the rod length: it decreases with an increase in L (for longer rods, the ordering starts earlier). The ω_{bif} value also depends on the lateral interaction parameter ε: an increase in the molecular attraction results in earlier ordering. The obtained distributions[25] are indicative of an important role of the ordering effect of molecules along their longer axes in the pattern of molecular distribution.

Below we consider distributions ordered along the X axis. All calculations were carried out at $T = 300$ K. The interaction energy of neighboring contacts ε varied from zero to 1260 J mol^{-1}, which falls into the characteristic region of the interaction energies of molecules in the absence of specific contributions to the intermolecular interaction. The ratio of the transition state energy to the ground state energy is $\alpha = \varepsilon^*/\varepsilon = 0.55$ (all contacts of the rod are energetically equivalent). The concentration dependences of the dynamic characteristics are normalized to their value for the rarefied gas in the bulk phase.

The transport coefficients of labeled molecules with different orientations in the bulk phase for rods of different lengths L are shown in Fig. 2. The dependences of these coefficients on the fluid density for rods of different sizes are presented in Fig. 2, *a*. The effect of ordering is manifested for all of the rod sizes considered, in particular, the concentration dependence of the coefficient is separated into two branches in the bifurcation point,[25] the upper branch describing the motion of the longer axis of the rod along the ordering axis X, which corresponds to the coefficient D_l^{XX} and the lower branch describing the motion of the longer axis of the rod across the X axis, which corresponds to the coefficients $D_l^{YY} = D_l^{ZZ}$. As the rod length L increases, the label transport coefficient rapidly decreases and the bifurcation point shifts to lower densities.

The influence of the lateral interaction parameter ε on the concentration dependences D_l^{XX} and D_l^{YY} is shown in Fig. 2, *b*. A stronger attraction between the molecules holds them together and decreases the transport coefficients of labeled molecules (in the general case, the pattern of the curves is also influenced by the parameter α). As in Fig. 2, *a*, the upper branch corresponds to D_l^{XX} and the lower branch, to $D_l^{YY} = D_l^{ZZ}$.

Analogous curves for the second type of motion, *i.e.*, across the longer axis of the rods, are presented in Fig. 2, *c*. The upper branches of the curves correspond to the coefficients $D_l^{YX} = D_l^{ZX}$ along the X axis, while the lower branches show coefficients of motion across the X axis. In the case of zero lateral interactions ($\varepsilon = 0$), $D_l^{XY} = D_l^{ZY}$.

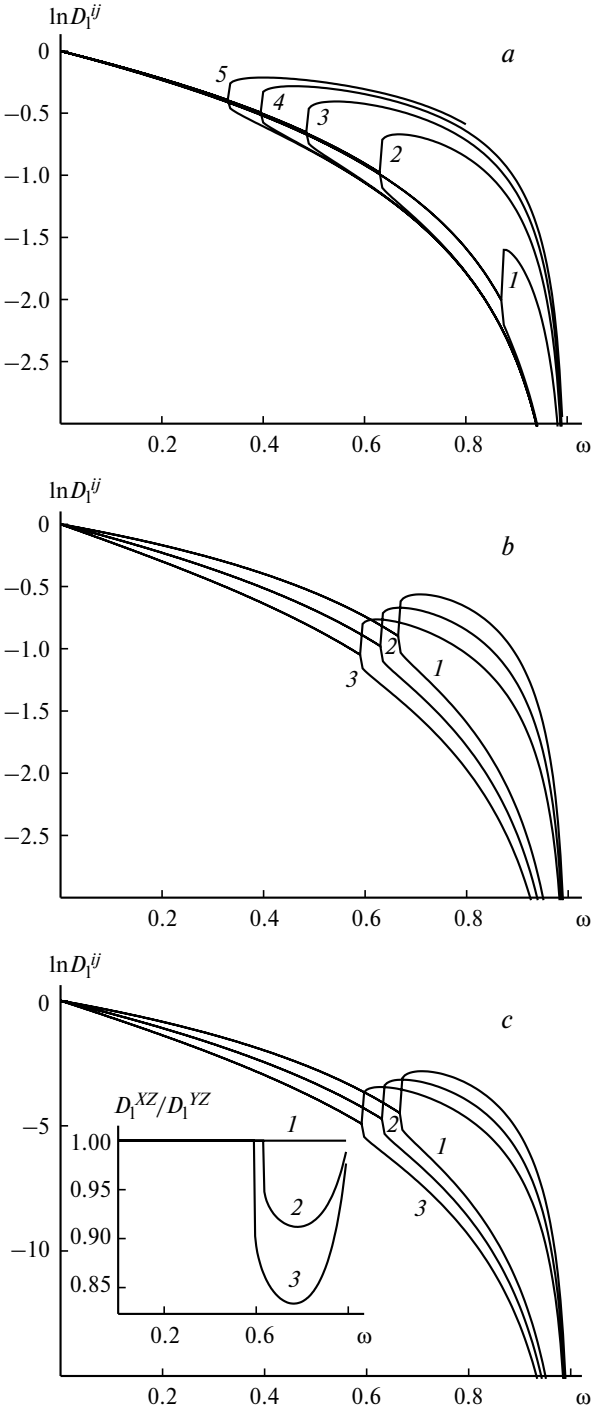

Fig. 2. Dependences of $\ln D_l^{ij}$ for rod movement along (*a*, *b*) and across (*c*) the longer axis on the volume fraction of the fluid ω for rods with the length $L = 4$ (*1*), 5 (*2*), 6 (*3*), 7 (*4*), 8 (*5*) for $\varepsilon =$ 420 J mol^{-1} (*a*) and for variation of the parameter $\varepsilon = 0$ (*1*), 420 (*2*), 840 J mol^{-1} (*3*) for rods with the length $L = 5$ (*b*, *c*). The inset shows the ratio of the coefficients D_l^{XZ}/D_l^{YZ} for $L = 4$ (*1*), 5 (*2*), and 6 (*3*).

As the concentration increases, the second type transport coefficients decrease much faster than the first type coefficients. Since the motion coefficients of molecules arranged along the *Y* and *Z* axes and across the *X* axis differ little from one another, then Fig. 2, *c* gives the curves corresponding to $D_l^{ZY} = D_l^{YZ}$ while the inset shows the D_l^{XZ}/D_l^{YZ} ratio. The coefficient for the second type motion of the rod arranged along the *X* ordering axis is greater than the coefficient for the corresponding motion of the rod arranged across the *X* axis.

Monolayer system. In the presence of a uniform solid surface, the difference between the binding energies ΔQ of horizontal and vertical rods is an important molecular characteristic of adsorption systems. The monolayer adsorption was calculated using the value $\Delta Q = 840$ J mol^{-1} per contact. The surface was assumed to be practically smooth and the activation energy along the surface was considered to be low. The label transport coefficient for the rods with $L = 6$ for the first type of motion and different intermolecular interactions ε are shown in Fig. 3. The upper branches of curves *2* and *3* correspond to the coefficient D_l^{XX} (rod movement along the ordering axis) and the lower branches correspond to $D_l^{YY} = D_l^{ZZ}$ (rod movement across the ordering axis). Under these conditions in the absence of lateral interactions between the molecules, no ordered arrangement of molecules[25] is observed. The greater the attraction between the molecules, the faster the label transport coefficient decreases with an increase in the coverage. For higher coverages, the vertical orientation of the rods starts to predominate[25] and both branches coincide.

Slit-shaped pores. In slit-shaped pores, the potential of both walls has an influence on the pattern of molecule orientations.[25] As the total concentration changes, the molecules can change orientation. The calculations were carried out for $H = 9$ monolayers and the rod length $L = 4$. The potential of each wall was considered equal to that on an open surface with $\Delta Q = 840$ J mol^{-1}.

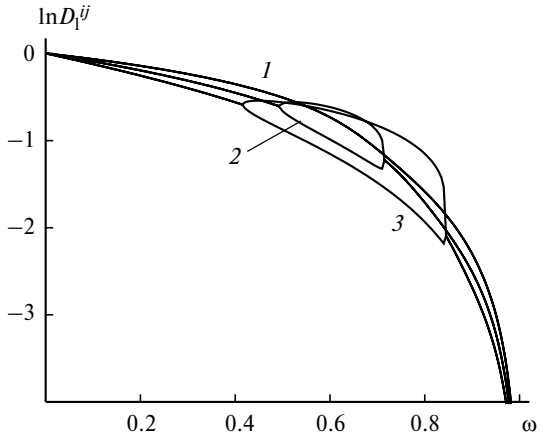

Fig. 3. Dependences $\ln D_l^{ij}$ for rod movement along the longer axis on the volume fraction of the fluid ω in the surface monolayer on variation of the parameter $\varepsilon = 0$ (*1*), 420 (*2*), 840 J mol^{-1} (*3*) for rods with $L = 6$.

Figure 4, *a* shows the transport coefficients for labeled molecules D_l^{ij} during their thermal motion from the pore second monolayer (q = 2) in different directions along (*1—3*) and across (*4—9*) the longer axis of the rod. The concentration dependences of the transport coefficients D_l^{ij} differ according to the type and direction of motion. This demonstrates the anisotropy of molecule motion as regards both the orientations and the directions. These differences are especially pronounced in the case of ordered distribution of molecules at high filling degrees of a pore: the curves are split with respect to the ordering axis.

The influence of the position of molecule on the concentration dependences of the label transport coefficients for movement along the X axis is illustrated by Fig. 4, *b*. The numbers of the curves correspond to the numbers in Fig. 4, *a*; therefore, no lower branches are shown in Fig. 4, *b*. Note that with an increase in the layer number, the point reflecting the ω_{bif} value moves monotonically from the ω_{bif} value in the first surface monolayer to the ω_{bif} value in the central layer, the latter being close to that for bulk phase. This is indicative of the crucial role of the concentration factor in the ordered arrangement of molecules. The wall potential creates a nonuniform distribution of molecules of different orientations along the normal to the wall, which results in a substantial dependence of the transport coefficients on the position of molecule.

Finally, Fig. 4, *c* shows the concentration dependences $\ln D_l^{ij}$ on ω for various energies of attraction between the molecules, which are characterized by the parameter ε. It can be seen that, apart from the motion direction and the ordering axis direction, the concentration dependences of the label transport coefficient are affected by the lateral interaction parameter. An increase in this parameter implies greater attraction between the neighboring molecules, which retards the label transport and results in an essential decrease in the transport coefficients.

Generally, Fig. 4 demonstrates that the concentration dependences of transport coefficients for rod-like molecules are much more complex than analogous dependences for small spherical molecules, which also depend, in narrow pores, on the distance from the pore wall and on the motion direction.[9,10,29]

Rotational motion coefficient of the label. The average angular rate of the rotational motion (or the rotation frequency) will be designated by w_f^i; it is related to the average jump rate $W_f(i\to k)$ as $w_f^i = \varphi W_f(i\to k)/\theta_f^i$.

For the rotational motion, a similar rotational diffusion coefficient of the label can be introduced. This coefficient characterizes the thermal rate of particle reorientation between different orientation states under equilibrium conditions. By analogy with expression (7), one can

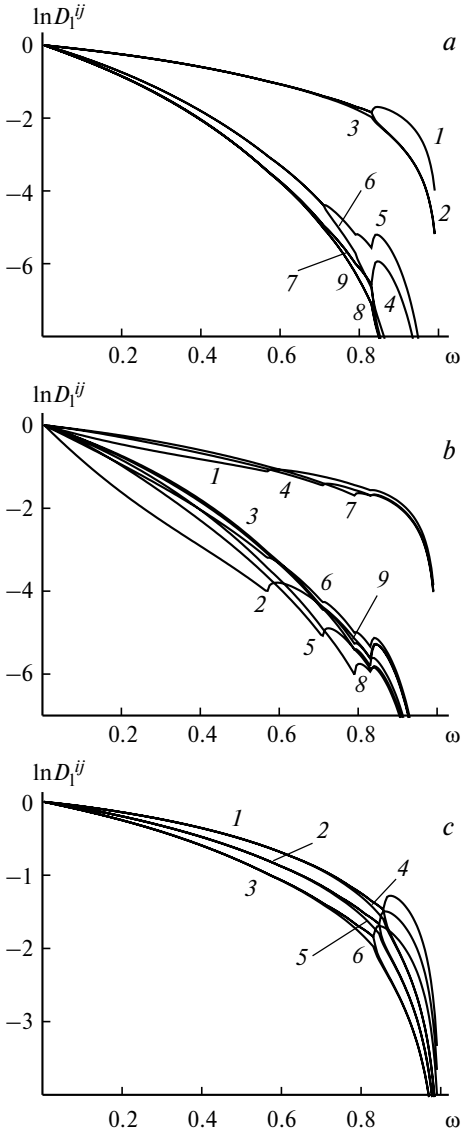

Fig. 4. (*a*) Dependences of $\ln D_l^{ij}$ on the volume fraction of the fluid ω in the second layer (q = 2) of a slit-shaped pore at α = 0.55, ε = 840 J mol^{-1}, L = 4, H = 9: rod movement along (*1—3*) and across (*4—9*) the longer axis; $\ln D_l^{ij}$, $i = j$ = X (*1*), Y (*2*), Z (*3*); $j = X$, $i = Y$ (*4*), Z (*5*); $j = Y$, $i = Z$ (*6*), X (*7*); $j = Z$, $i = X$ (*8*), Y (*9*). (*b*) dependences of $\ln D_l^{ij}$ on the volume fraction of the fluid ω in different layers of a slit-shaped pore at α = 0.55, ε = 840 J mol^{-1}, L = 4, H = 9. Transport coefficients D_l^{iX} in the first (*1—3*), second (*4—6*), and third (*7—9*) layers of a pore; the numbers of the curves correspond to the numbers given in Fig. 4, *a*. For $i = X$, transport of molecules according to the first type of motion, for $i \neq X$, according to the second type of motion. (*c*) $\ln D_l^{ii}$ for the movement of molecules along their longer axes in the central layer of a slit-shaped pore *vs.* the fluid volume fraction ω for α = 0.55, L = 4, H = 9; curves *1—3* show the movement coefficients in the tangential direction relative to the pore axis; the upper branch corresponds to D_l^{XX}, the lower branch, to D_l^{YY}, and curves *4—6* are the movement coefficients D_l^{ZZ} in the lateral direction relative to the pore axis for ε = 0 (*1*, *4*), 420 (*2*, *5*), and 840 J mol^{-1} (*3*, *6*).

derive the following equation for the rotational diffusion coefficient of the label:

$$D_f^{i*} = z_f^*(i\to k)\varphi^2 W_f(i\to k)/\theta_f^i, \qquad (8)$$

where $z_f^*(i\to k)$ is the number of possible rotations between states $i\to k$ for site f. If "direct" rotations occur, then according to the above-accepted definition of sorts of particles, $z_f^*(i\to k) = 1$. The dimension of the rotational diffusion coefficient is rad^2 s^{-1}.

Let us designate the label transport coefficient for the rotational diffusion by D_r^{ij} with superscripts i and j characterizing the initial and final orientations of the rod. Rotation is considered only for the cases where $i \neq j$.

The concentration dependences of the rotational diffusion coefficients of rod-like molecules with the length $L = 5$ in the bulk phase for various lateral interaction parameters ε are presented in Fig. 5. As the attraction of molecules increases, their ordering appears at lower density.

Since rotation is possible only in the presence of a vacancy region larger than that required for the translational motion of molecules, the attraction of neighboring molecules, which promotes aggregation, makes this process less probable. This can be clearly seen from comparison of the typical variation range of the transport coefficient from low to high densities (see Figs. 1—3, 5, ordinate scale).

The probability of existence of large vacancy regions is related to the rotation direction with respect to the ordering axis. Thus, the rotational diffusion coefficients for the rotation of a molecule along the ordering direction $D_r^{YX} = D_r^{ZX}$ (the upper branches of the curves) differ appreciably from the rotational diffusion coefficients across this direction $D_r^{YZ} = D_r^{ZY}$ (the lower branches of the curves). As a consequence, transition of the fluid into an ordered state enhances the differences between the coefficients corresponding to rotations along and across the ordering axis of rod-like molecules.

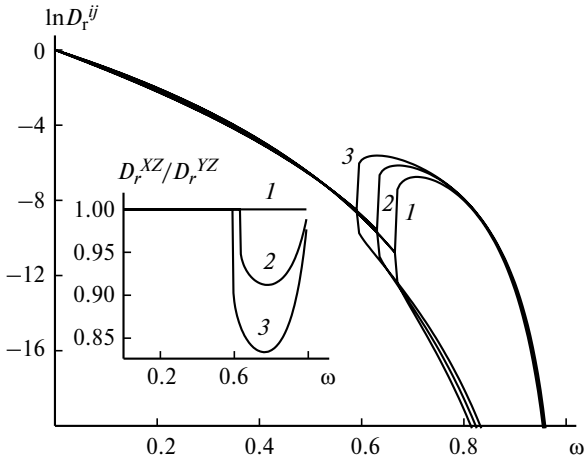

Fig. 5. Rotational diffusion coefficients D_r^{ij} of rod-like molecules with $L = 5$ *vs.* the fluid volume fraction ω in the bulk phase for the lateral interaction parameter ε = 0 (*1*), 420 (*2*), and 840 J mol^{-1} (*3*). The inset shows the ratio of the coefficients D_r^{XZ}/D_r^{YZ} (for rods lying along and across the *X* axis) the difference between which is barely seen in the presented plot due to the too small scale.

Shear viscosity coefficient. The expression for the local viscosity coefficient η_{fg} for shear of a mixture of molecules in site g relative to site f (here $\chi = 1$, therefore, this index is omitted) has the form

$$\eta_{fg} = \left[\sum_{j=1}^{s-1} x_j \left(\eta_{fg}^j\right)^{-1}\right]^{-1}, \qquad \eta_{fg}^j = \theta_f^j / U_{fg}^{iv}, \qquad (9)$$

$$x_f^j = \theta_f^j/\theta_f, \qquad \theta_f = \sum_{i=1}^{s-1} \theta_f^i,$$

where x_f^j is the mole fraction of component j in site f; θ_f is the complete filling of site f; the expression for the thermal migration rate $U_{fg}^{iv}(\chi = 1)$ was defined above.

The shear viscosity coefficient in the bulk phase for rods with length $L = 5$ is shown in Fig. 6, *a*. As the fluid density increases, the coefficient increases. The ordering effect depends substantially on the interaction between

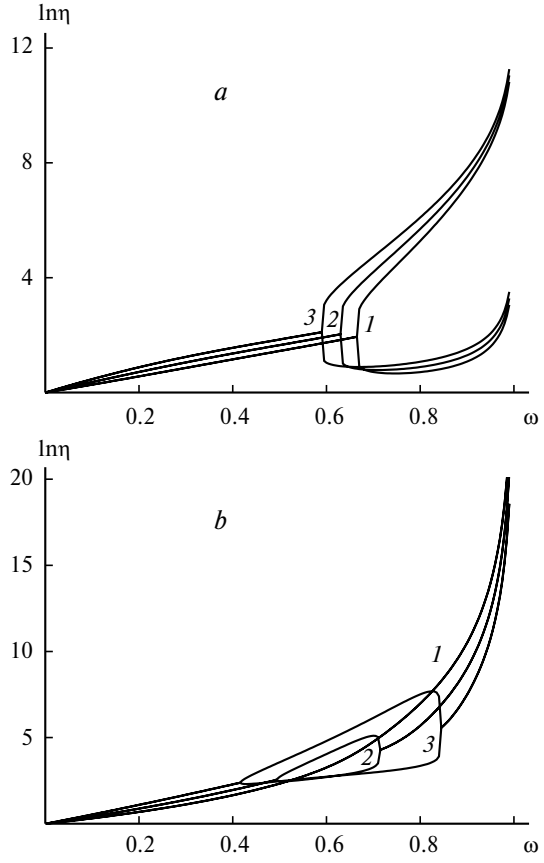

Fig. 6. Shear viscosity coefficient lnη *vs.* the fluid volume fraction ω in the bulk phase for rods with $L = 5$ (*a*) and 6 (*b*) for ε = 0 (*1*), 210 (*2*), 420 J mol^{-1} (*3*).

the molecules ε. The upper and lower branches of the curves correspond to the viscosity across and along the fluid ordering axis, respectively. The shear viscosity coefficient along the ordering axis is lower in an ordered phase than in a disordered phase.

The same behavior of the shear viscosity coefficient is observed in the case of monolayer adsorption of rods with $L = 6$ (see Fig. 6, *b*). The lower branches of the curves correspond to the viscosity along the ordering axis, while upper branches correspond to the perpendicular direction with respect to ordering axis (in the monolayer plane).

Slit-shaped pores. As above, calculations for the slit were carried out for $H = 9$ monolayers and rod length $L = 4$. Dependences of the shear viscosity coefficient for different directions of rod movement are shown in Fig. 7, *a* ($i = X, Y, Z$ shows the movement direction). Curves *1—3* describe the coefficients for movement components in the *XY* plane, curves *4—6* correspond to the vertical movement component *Z*. The orderings within each *XY* layer separate the components: the lower branch $i = X$ corresponds to the direction along the ordering axis, while the upper branch $i = Y$ corresponds to the direction across the ordering axis.

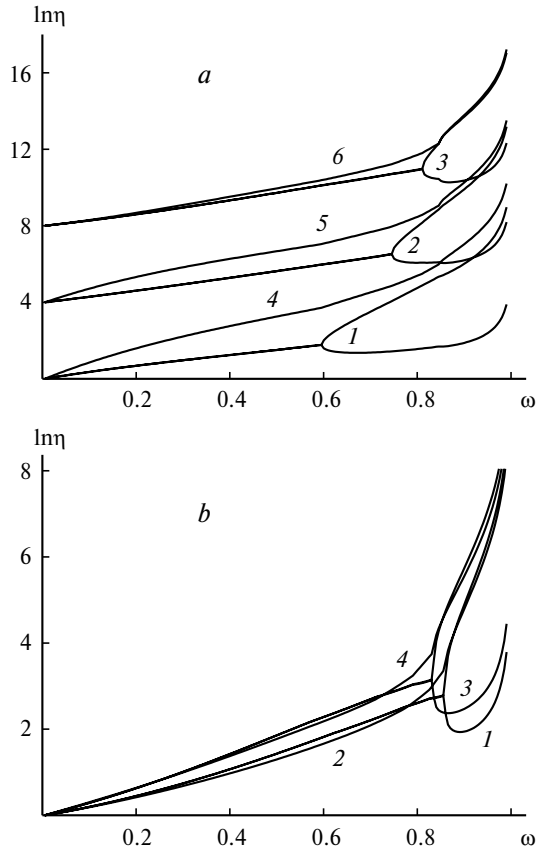

Fig. 7. Shear viscosity coefficient lnη *vs.* the fluid volume fraction ω in a slit-shaped pore $H = 9$ for $L = 4$ at a constant (*a*) or variable (*b*) parameter ε; *a*. Movements in the *XY* plane (*1—3*) and along the *Z* direction (*4—6*); the curves are consecutively shifted by four sites: the first (*1*, *4*), second (*2*, *5*), and third (*3*, *6*) monolayers; *b*. The parameter ε = 0 (*1*, *2*), and 420 (*3*, *4*) J mol^{-1}.

The general pattern of the curves coincides; however, one can see that ordering first takes place in the first layer, then in the second layer, and after that, in the third layer. As the layer number increases, the difference between branches *X* and *Y* becomes more pronounced. The influence of the wall potential is visible even at low filling degrees of the pore.

The effect of the intermolecular interaction on the concentration dependences of the viscosity coefficient for various movement directions in the third monolayer counted off from a pore wall (the two walls are equivalent) is presented in Fig. 7, *b*. The upper branches of curves *1* show the variation of the viscosity along the *Y* direction, while lower branches, along the *X* direction. Curves *2*, *4* demonstrate how the viscosity varies along the *Z* direction. The stronger the attraction between the molecules, the faster the viscosity coefficient increases with the progress of bulk filling of the pore. In this case, the divergence between the viscosity coefficients of the two branches within a layer decreases with an increase in ε due to predominance of the contribution of the intermolecular interactions over the effect of the wall potential.

* * *

The performed calculations indicate that label translational and rotational transport coefficients and the shear viscosity coefficients depend substantially on the concentration of molecules in the fluid. Unlike the analogous curves for spherical molecules, these curves have kinks associated with ordering of molecule orientation along their longer axes. This gives rise to nonmonotonic dependences of these dynamic characteristics on the concentration.

The coefficients we found can be used for a self-consistent description of fluxes of labeled particles over a broad range of concentrations and temperatures including the region of phase transitions, in particular, the critical region. Thus, these coefficients can be used to calculate fluxes under capillary condensation conditions of particles in narrow pores. The values of the coefficients are consistent with the known values that follow from the molecular kinetic theory for gas mixtures at very low concentrations ($\theta \approx 10^{-4}$—10^{-3}) and for liquids ($\theta \approx 1.0$), and they also properly reflect the temperature behavior of the kinetic coefficients in rarefied gas and liquid mixtures.[18]

In this study we used an averaged description of the influence of neighboring molecules on the dynamics of elementary thermal migrations of the molecule. This approach provides a reliable concentration dependence of the migration and rotation rates for a single-component fluid of rod-like molecules and for dense phases in multicomponent mixtures of rods. The case of gas type densi-

ties of the mixtures of rod-like molecules requires a more detailed consideration: to reach agreement with the strict kinetic gas theory, the collisions of molecules with their neighbors should be explicitly taken into account.[29]

This work was financially supported by the Russian Foundation for Basic Research (Project No. 03-03-32072a).

References

1. D. P. Timofeev, *Kinetika adsorbtsii* [*Adsorption Kinetics*], Izd-vo AN SSSR, Moscow, 1962, 252 pp. (in Russian).
2. C. N. Satterfield, *Mass Transfer in Heterogeneous Catalysis*, MIT Press, Cambridge (Mass.), 1970.
3. E. A. Mason and A. P. Malinauskas, *Gas Transport in Porous Media: The Dusty-Gas Model*, Elsevier, Amsterdam, 1983.
4. Yu. K. Tovbin, in *Sovremennoe sostoyanie i perspektivy razvitiya teorii adsorbtsii (Materialy konferentsii, posvyashchennoi 100-letiyu M. M. Dubinina)* [*Current State and Prospects of Development of the Adsorption Theory (Proc. Conf. Dedicated to the 100th Anniversary of M. M. Dubinin´s Birthday)*], Institute of Physical Chemistry of the RAS, Moscow, 2001, 27 (in Russian).
5. B. D. Todd and D. J. Evans, *J. Chem. Phys.*, 1995, **103**, 9804.
6. J. M. D. MacElroy, *J. Chem. Phys.*, 1994, **101**, 5274.
7. B. J. Palmer, *J. Chem. Phys.*, 1998, **109**, 196.
8. Yu. K. Tovbin, *Metod moleculeyarnoi dinamiki v fizicheskoi khimii* [*Molecular Dynamics in Physical Chemistry*], Nauka, Moscow, 1997, 128 (in Russian).
9. Yu. K. Tovbin, *Khim. Fiz.* [*Chem. Phys.*], 2002, **21**, No. 1, 83 (in Russian).
10. Yu. K. Tovbin, *Zh. Fiz. Khim.*, 2002, **76**, 76 [*Russ. J. Phys. Chem.*, 2002, **76** (Engl. Transl.)].
11. Yu. K. Tovbin, *Teoriya fiziko-khimicheskikh protsessov na granitse gaz—tverdoe telo* [*Theory of Physicochemical Processes at the Gas—Solid Interface*], Nauka, Moscow, 1990, 288 pp. (in Russian).
12. Yu. K. Tovbin, *Progress in Surface Science*, 1990, **34**, No. 1—4, 1.
13. N. A. Smirnova, *Molekulyarnaya teoriya rastvorov* [*Molecular Theory of Solutions*], Khimiya, Leningrad, 1987, 360 pp. (in Russian).
14. S. Chandrasekhar, *Liquid Crystals*, Cambridge Univer. Press, Cambridge, 1977.
15. I. P. Bazarov and E. V. Gevorkyan, *Statisticheskaya teoriya tverdykh i zhidkikh crystalov* [*Statistical Theory of Solid and Liquid Crystals*], Izd. MGU, Moscow, 1983, 262 pp. (in Russian).
16. Yu. K. Tovbin, *Izv. Akad. Nauk. Ser. Khim.*, 1999, 1467 [*Russ. Chem. Bull.*, 1999, **48**, 1450 (Engl. Transl.)].
17. Yu. K. Tovbin, L. K. Zhidkova, and V. N. Komarov, *Izv. Akad. Nauk. Ser. Khim.*, 2001, 752 [*Russ. Chem. Bull., Int. Ed.*, 2001, **50**, 786].
18. J. O. Hirschfelder, C. F. Curtiss, and R. B. Bird, *Molecular Theory of Gases and Liquids*, Wiley, New York, 1954.
19. A. V. Kiselev, *Mezhmoleculyarnye vzaimodeistviya v adsorbtsii i khromatografii* [*Intermolecular Interactions in Adsorption and Chromatography*], Vysshaya shkola, Moscow, 1986, 360 pp. (in Russian).
20. W. A. Steele, *The Interactions of Gases with Solid Surfaces*, Pergamon, New York, 1974.
21. Yu. K. Tovbin, *Dokl. Akad. Nauk*, 1995, **345**, 639 [*Dokl. Chem.*, 1995 (Engl. Transl.)].
22. Yu. K. Tovbin, *Khim. Fiz.* [*Chem. Phys.*], 1997, **16**, No. 6, 96 (in Russian).
23. Yu. K. Tovbin and E. V. Votyakov, *Kinet. Katal.*, 1998, **39**, 733 [*Kinet. Catal.*, 1998, **39** (Engl. Transl.)].
24. Yu. K. Tovbin, *Zh. Fiz. Khim.*, 2005, **80**, 995 [*Russ. J. Phys. Chem.*, 2005, **80** (Engl. Transl.)].
25. Yu. K. Tovbin and A. B. Rabinovich, *Izv. Akad. Nauk. Ser. Khim.*, 2006, 1476 [*Russ. Chem. Bull., Int. Ed.*, 2006, **55**, 1530].
26. E. A. Moelwyn-Hughes, *Physical Chemistry*, Pergamon Press, London—New York—Paris, 1961.
27. S. Glasston, K. J. Laidler, and H. Eyring, *The Theory of Rate Processes*, Princeton University, New York, 1941.
28. L. D. Landau and E. M. Lifshits, *Teoreticheskaya fizika. I. Mekhanika* [*Theoretical Physics. I. Mechanics*], Nauka, Moscow, 1965, 204 pp. (in Russian).
29. Yu. K. Tovbin, *Izv. Akad. Nauk. Ser. Khim.*, 2005, 1717 [*Russ. Chem. Bull., Int. Ed.*, 2005, **54**, 1768].

Received December 21, 2005;
in revised form August 31, 2006